Comparative functional study of the viral telomerase RNA based on natural mutations

Laëtitia Fragnet, Emmanuel Kut, Denis Rasschaert

THE JOURNAL OF BIOLOGICAL CHEMISTRY
Vol. 280, No. 25, Issue of June 24, pp. 23502–23515, 2005

Printed in U.S.A.

Comparative Functional Study of the Viral Telomerase RNA Based on Natural Mutations*

Received for publication, February 1, 2005, and in revised form, March 23, 2005
Published, JBC Papers in Press, April 4, 2005, DOI 10.1074/jbc.M501163200

Laetitia Fragnet, Emmanuel Kut, and Denis Rasschaert‡

From the Laboratoire Telomerase, Lymphome Viro-induit, Centre de Recherches INRA de Tours, UR-BASE 086, 37380 Nouzilly, France

Telomerase activity is present in most malignant tumors and provides a mechanism for the unlimited potential for division of neoplastic cells. We previously characterized the first identified viral telomerase RNA (*vTR*) encoded by the Marek's disease virus (MDV) (Fragnet, L., Blasco, M. A., Klapper, W., and Rasschaert, D. (2003) *J. Virol.* 77, 5985–5996). This avian herpesvirus induces T-lymphomas. We demonstrated that the vTR subunit of the oncogenic MDV-RB1B strain is functional and would be more efficient than its chicken counterpart, cTR, which is 88% homologous. We take advantage of the functionality of those natural mutant TRs to investigate the involvement of the mutations of *vTR* on its efficiency in a heterologous murine cell system and in a homologous *in vitro* system using the recombinant chicken telomerase reverse transcriptase. The P2 helix of the pseudoknot seems to be more stable in vTR than in cTR, and this may account for the higher activity of vTR than cTR. Moreover, the five adenines just upstream from the P3 helix of *vTR* may also play an important role in its efficiency. We also established that the substitution of a single nucleotide at the 3′-extremity of the H-box of the vaccine MDV-Rispens strain *vTR* resulted in a lack of its accumulation within the cell, especially in the nucleus, correlated with a decrease in telomerase activity.

Telomeres are nucleoprotein structures found at the extremities of eukaryotic linear chromosomes (1). They are essential for chromosome stability, and thus, genome rearrangements, the cell cycle, and carcinogenesis depend directly on the integrity of these structures (2). Telomeres are composed of tandemly repeated DNA sequences, which consist of 5′-GGTTAG-3′ hexamers in vertebrates. Telomeres replicate by a specific mechanism involving telomerase, a ribonucleoprotein complex that serves as the preferential system for compensating the erosion of telomeres at each round of DNA replication (3). The minimal telomerase complex sufficient for *in vitro* activity comprises two major components: 1) a protein subunit (TERT)[1] with reverse transcriptase activity associated with 2) an RNA subunit (TR) containing a short template sequence specific for telomere repeats (4). Telomerase activity is tightly regulated in cells. According to the constitution of the minimal telomerase complex, the regulation of the telomerase activity would rest on either the expression of the TERT or the TR subunits, as described in human or mouse, respectively. In addition, telomerase is not detectable in normal somatic cells but is strongly expressed during fetal development and constitutively expressed in highly proliferative postnatal cells such as germ line cells, stem cells, and lymphocytes (5, 6). Furthermore, high levels of telomerase activity are also detected in a large range of cancers (at least 85%) and are closely associated with immortalization processes (7, 8).

In the last three years, a correlation has been established between telomerase activity and viral infections with the oncogenic papillomavirus HPV16 (9) and the herpesviruses HHV8 (10) and Epstein-Barr virus (11). However, although infections with these viruses are accompanied by an increase of telomerase activity in cells, none of these viruses has been demonstrated to encode a telomerase component. The avian Marek's disease virus (MDV), which induces malignant T lymphomas in chickens, is therefore currently the only virus among oncogenic and non-oncogenic viruses that encodes a telomerase RNA subunit gene (*vTR*) (12). It is worth stating that the *vTR* gene is specifically present in the genome of the strains of the GaHV2 serotype, including all of the known oncogenic strains of MDV such as the MDV-RB1B strain from which *vTR* was isolated, and the non-oncogenic vaccine strain MDV-Rispens (12). The MDV-RB1B *vTR* is a 443-bp gene that displays as its avian counterpart, *cTR*, the eight conserved regions (CR1–CR8) common to all vertebrate TRs, as shown by phylogenetic analysis (Fig. 1). These regions delimit the three main structural domains of TRs (12, 13). The template-pseudoknot domain is essential for telomerase activity. It consists of the template sequence that is reverse-transcribed by the protein component (TERT) and the pseudoknot domain, which constitutes one of the two sites of interaction between the TR and TERT subunits (14). The essential role of the CR1 domain as a template has been clearly demonstrated (15, 16), but the sequences flanking this conserved region are also important because the four nucleotides immediately downstream from the CR1 region play a key role in aligning TR on telomere sequences, possibly strengthening the processivity of the telomerase complex (17). A recent study (18) has shown that the telomerase complex would function as a multimer and that the pseudoknot domain is involved in TR dimerization and interaction with TERT. The dimerization interface would consist of the P3 helix generated from the CR2 region of one TR molecule base-paired with the CR3 region of a second TR molecule. The integrity of the primary sequence and secondary structure of the P2 and P3 helices and thus that of the sequences of the CR2 and CR3 regions, which are composed of these stems, are

* This work was supported by grants from the "Ligue Nationale Contre le Cancer" and the "Région Centre." The costs of publication of this article were defrayed in part by the payment of page charges. This article must therefore be hereby marked "*advertisement*" in accordance with 18 U.S.C. Section 1734 solely to indicate this fact.

‡ To whom correspondence should be addressed: Laboratoire Telomerase, Lymphome Viro-induit, UR086, INRA, Centre de Recherches de Tours, 37380 Nouzilly, France. Tel.: 33-247-427-942; Fax: 33-247-427-774; E-mail: rasschae@tours.inra.fr.

[1] The abbreviations used are: TERT, telomerase reverse transcriptase; TR, telomerase RNA; vTR, viral TR; hTR, human TR; cTR, chicken TR; chTERT, chicken TERT; mTR, murine TR; RT-PCR, reverse transcriptase-PCR; MDV, Marek's disease virus; WT, wild type; RACE, rapid amplification of cDNA ends; CR, conserved region.

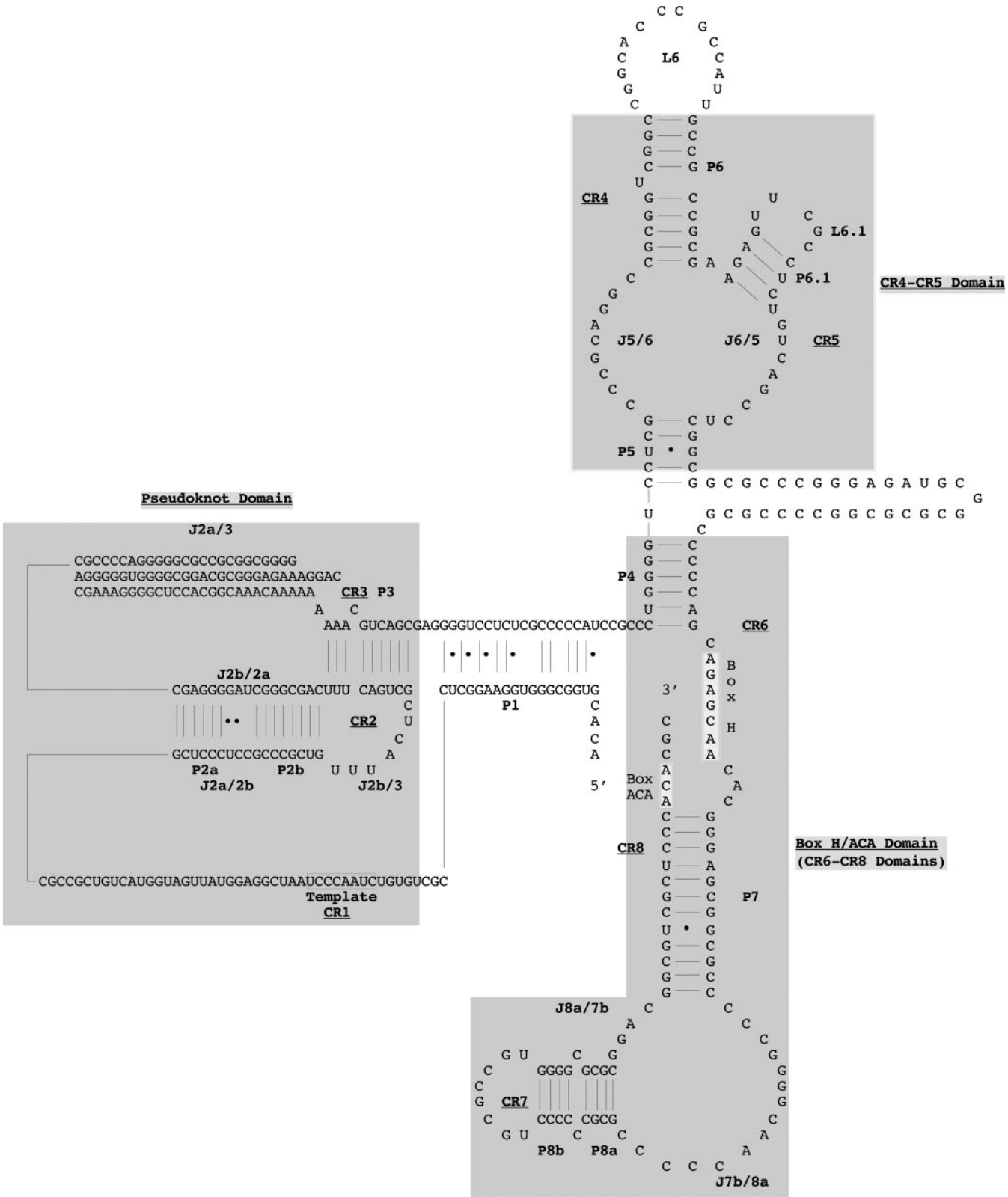

FIG. 1. **Proposed secondary structure of the Marek's disease virus telomerase RNA.** The overall proposed secondary structure of vTR is based on the vertebrate TR structure published by Chen *et al.* (10). Paired regions (*P*) are numbered from 5′ to 3′ as P1–P8. Junction regions (*J*) between two paired regions are named with reference to the flanking paired regions. The three universal structural domains conserved in all of the vertebrate TRs are *shaded* in *gray* and *labeled*. The template region, H-Box, and Box ACA motifs are labeled, and their conserved nucleotides are *boxed*. Universal base pairing (according to Watson-Crick) is represented by *dashes*, whereas G/U pairs and non-canonical A/C pairs are shown by *squares* and *circles*, respectively.

essential to the functionality of the "pseudoknot domain" (19). The pseudoknot is also important because it is able to interact with TERT. Indeed, the association of this domain with the second functional domain CR4/CR5 is sufficient to reconstitute a telomerase activity *in vitro* (14). Recent functional studies based on the hTR model identified various sites of interaction

between hTERT and hTR. The RT motifs of TERT seem to interact with sequences in the vicinity of the CR1 region of hTR, and both the C-terminal and RID1 domains responsible for TERT catalytic activity and the processivity of the complex seem to interact preferentially with the "pseudoknot domain." Moreover, the CR4/CR5 domain of hTR and the P6.1 helix of this domain, in particular, have been shown to constitute the second point of anchorage between TR and TERT via the essential DNA synthesis domain, RID2 (18). The third domain, the H/ACA CR7 domain, is dispensable for *in vitro* telomerase activity but essential for TR activity *in vivo*. Indeed, this domain is involved in the nuclear and nucleolar targeting of TR, resulting in 3′-end processing and their intracellular stability (20, 21). The relevance of this domain was illustrated by studies on the dyskeratosis congenital disorder affecting especially the bone marrow and skin. Telomere length seems to be significantly shorter than normal in patients with this rare inherited disorder and is associated with a lack of telomerase activity. Three forms of congenital dyskeratosis have been described (22, 23), of which the autosomal dominant form is the most severe. This form of the disease is characterized by mutations in the *hTR* gene and, in particular, the deletion of the H/ACA CR7 domain of hTR, which is responsible for the lack of telomerase activity due to failure of accumulation of the TR.

We have shown previously (12) that the *vTR* gene sequence is 88% homologous to that of the chicken *cTR* gene. Alignment of the sequences of these two genes showed that the CR was entirely conserved, and with the exception of a one-nucleotide deletion in the CR2 region of *vTR*, the main sequence divergences essentially concerned the junction region of the pseudoknot domain. This is of particular importance, because these mutations would be implicated in an increase of the vTR efficiency because this viral TR would reconstitute a 6-fold higher cellular telomerase activity than its chicken counterpart (12). Although the *vTR* gene of the oncogenic MDV-RB1B strain presents H-Box, ACA-Box, and CR7 domain consensus sequences identical to those of vertebrate TRs, one of the three point mutations identified in the *vTR* gene of the vaccine MDV-Rispens strain affects the 3′-end of the H-box (12).

Here we report a functional dynamics study based on differences in efficiency between TRs sharing high sequence conservation. We investigated the 12% nucleotide sequence divergence resulting in differences in telomerase activity (by a factor of six) between vTR and cTR to identify the mutations responsible for increasing the efficiency of vTR over that of cTR. We also investigated the functional significance of the mutations in the *vTR* gene of the non-oncogenic MDV-Rispens strains by comparing this gene with the *vTR* of the oncogenic MDV-RB1B strain. For both parts of the study, we used a murine heterologous cell system, making it possible to assess both functional activity and accumulation of the mutated TR in cells, and then we performed an *in vitro* approach, allowing free accumulation constraints to assess the functionality of the TR with the homologous avian telomerase protein component, chTERT.

MATERIALS AND METHODS

Cell Line—We used a murine heterologous cell system, the KO3p23mTR$^{-/-}$ cell line, which consists of immortalized murine fibroblasts lacking telomerase activity due to the knocking out of the murine telomerase RNA gene (*mTR*). This cell line, kindly provided by Maria A. Blasco (24), was cultured in Dulbecco's modified Eagle's medium (Cambrex) supplemented with 10% fetal bovine serum (Sigma) at 37 °C in an atmosphere containing 5% CO_2.

Expression Constructs—The wild-type *vTR* and *cTR* genes previously cloned under the control of the cytomegalovirus promoter in the pCDNA3 vector (Invitrogen) were used as a control in each experiment (12). The *vTR* gene of the vaccine MDV-Rispens strain (Fort-Dodge Santé Animale), amplified at the time of sequence analysis for the various MDV strains (12), was also cloned in this vector to generate the Risp construct.

Specific mutations were introduced into the *vTR* sequence by PCR amplification. We used two approaches to generate mutations, depending on the site within the gene. We introduced mutations at distal positions of the TR directly via the primer sequence used for amplification. This method was used to generate the dcpvfv-, TEM-, and ACAD-mutated TR constructs from the PBMB 8-5 clone (12) with primer pairs 900/790, 928/790, and 791/934, respectively (Table I). The HACAD construct was also obtained in this way with the 791/934 primer pair from the HD construct described below. We introduced internal mutations in TR (Mut23, 4pbc, 1pbc, T/Gc, G/Ac, J2/3D, J2/3M, HD, HRI, and HACABR constructs) and developed chimeric *vTR*/*cTR* (dvpvfc and dcpvfc constructs) constructs by means of overlap extension (25). We initially generated two fragments per mutated gene by PCR using two specific primer pairs, including two overlapping internal primers for the *vTR* sequence encompassing the mutation of interest. We then combined 50 ng of each purified PCR product in a second PCR using the outermost 5′- and 3′-oligonucleotides used in the first two PCR reactions to construct the desired mutated gene. The primers and templates used in this approach are shown in Tables I and II. It is noteworthy that the J2/3v/c construct was also obtained by overlap extension, but four different PCR fragments were required as indicated in Table II. The entire mutated TR molecules obtained with these two approaches were then purified and inserted into the pGEMTeasy cloning vector. They were then subcloned under control of the cytomegalovirus promoter into pCDNA3 digested with EcoRV/NotI. All of the intermediate and final constructs were sequenced with appropriate primers to check that the mutations of interest had been correctly introduced into the inserted fragment.

Cloning and Sequencing of the Chicken TERT cDNA—We isolated chTERT mRNA from thymus cells extracted from the PA-12 White Leghorn chicken line. We obtained chTERT cDNA by RT-PCR and nested PCR using oligonucleotides synthesized using a library developed by the University of Manchester Institute of Science and Technology, covering the entire chicken TERT sequence with the exception of the 5′-end. The 5′-distal fragment of the chTERT cDNA was obtained by RACE-PCR using a chicken testis full-length cDNA library (Seegene). All of the PCR products were gel-purified and inserted into the pGEMTeasy vector (Promega) for sequencing. The entire coding region of chTERT was then constructed from the PCR products and inserted into the pET-14b vector (Novagen) under the control of the inducible T7 promoter.

Transient Expression—The different mutated and wild-type TR constructs were expressed in the KO3 p23 mTR$^{-/-}$ cell line as previously described (12). Cells were plated in 100 mm-diameter dishes and transiently transfected with 20 μg of each pCDNA TR construct using the Lipofectin reagent according to the manufacturer's instructions (Invitrogen). After 6 h of incubation at 37 °C, fresh medium was added to each dish. The cells were harvested 48 h after transfection for the assessment of telomerase activity and the extraction of cellular and nuclear RNA.

DNA Template for T7 Transcription—DNA templates for the T7 *in vitro* transcription of telomerase RNA fragments were generated by PCR amplification as previously described (13) with the exception of the *cTR* gene. Indeed, because we were unable to amplify the complete *cTR* gene by PCR (12), the *cTR* gene was instead cloned under the control of the T7 promoter. We fused the *cTR* gene with the T7 promoter (in *boldface*) by introducing this promoter into the pBS SK− plasmid by direct cloning of the corresponding annealed 5′-phosphorylated oligonucleotides M109 (5′-PaattcCTGCAGCCAAGCTTC**TAATACGACTCACTATAGGGAGA***ACGCGT*CGTCA-3′) and M111 (5′-P*GACGCGT*-**TCTCCCTATAGTGAGTCGTATTA**GAAGCTTGGCTGC AGg-3′) (P in primers represents phosphorylated). Annealing was performed by heating for 10 min at 100 °C and cooling to 35 °C in a volume of 100 μl containing 5 nmol of each primer (20 mM Tris-HCl buffer, pH 7.4, and 200 mM NaCl) (26). We used the EcoRI (in *lowercase*) and PstI (*underlined*) sites present at the extremities of the annealed product for insertion of the fragment into the appropriately cut and dephosphorylated pBS SK− plasmid at a molar ratio of 5:1 (duplex:vector). The MluI/BamHI cTR fragment obtained by digestion of the pCMV *cTR* construct (12) was then inserted into the pBS-T7 plasmid cleaved with BamHI and MluI (in *italics* in the M109 and M111 primer sequences). For T7 *in vitro* transcription, the *cTR* gene was removed from the resulting construct by PstI digestion and purified from agarose gel (Ultrafree DA, Millipore).

The DNA template for T7 *in vitro* transcription of telomerase mutant and wild-type *vTR* genes was obtained by PCR amplification of pCDNA3 plasmid containing the gene of interest. The forward oligonucleotide M107 (5′-CCAAGCTTC**TAATACGACTCACTATAGGGAGA-**

TABLE I
Primers used to perform mutated TR

N°	Primers sequences [a]	Orientation
900	CGGACGCGTGGCGGGTGGAAGGCTCCGCTGTGCCTAACCCTAATCGGGGGAATTGATGGTGCTGTCGCCG	Forward
928	CGGACACGTGGCGGGTGGAAGGCTCCGCTGTG--------TAATCGGAGGTAT	Forward
934	CTGCAGGCG---GGGAGCGACGCCGTCCGCGCG	Reverse
767	CCGCATCTCCCGGGCGCCGC	Forward
770	GGCGTAGAGGGCCCGCGGCG	Reverse
901	GCGCTCCCTCCGCCCGCCCGCTGTTTTACTCGCTGACTTTCAGCGGGCGAGAGGAGCCGCC	Forward
902	CGCGAGGGAGGCGGGCGGGCGACAAAATGAGCGACTGAAAGTCGCCCGCTCTCCTCGGCGG	Reverse
904	TTGCAGTCGCTCCCCAGGAGAGCGGGGGTAGGCGGGACCCCAGG	Forward
905	AACGTCAGCGAGGGGTCCTCTCGCCCCCATCCGCCCTGGGGTCC	Reverse
907	AACGTCAGCGAGGGGTCCGCTCGCCCCGATCCGCCCTGGGGTCC	Forward
906	TTGCAGTCGCTCCCCAGGCGAGCGGGGCTAGGCGGGACCCCAGG	Reverse
910	GCGCTCCCTCCGCCCGCCCGCTGTTTACTCGCTGACTTTCAGCGGGCTAGGGGAGCCGCC	Forward
911	CGCGAGGGAGGCGGGCGGGCGACAAATGAGCGACTGAAAGTCGCCCGATCCCCTCGGCGG	Reverse
914	GCGCTCCCTCCGCCCGCTGTTTTACTCGCTGACTTTCAGCGGGCTAGGGGAGCCGCC	Forward
915	CGCGAGGGAGGCGGGCGACAAAATGAGCGACTGAAAGTCGCCCGATCCCCTCGGCGG	Reverse
918	GCGCTCCCTCCGCCCGCTGTTTACTCGCTGACTTTCAGCGGGCGAGGGGAGCCGCC	Forward
919	CGCGAGGGAGGCGGGCGACAAATGAGCGACTGAAAGTCGCCCGCTCCCCTCGGCGG	Reverse
922	GCGCTCCCTCCGCCCGCTGTTTACTCGCTGACTTTCAGCGGGCTAGAGGAGCCGCC	Forward
923	CGCGAGGGAGGCGGGCGACAAATGAGCGACTGAAAGTCGCCCGATCTCCTCGGCGG	Reverse
924	CGAAAGGGGCTCCGCGGC---C---AAAAAAACGTCAGCGAGGGGTC	Forward
925	GCTTTCCCCGAGGCGCCG---G---TTTTTTTGCAGTCGCTCCCCAG	Reverse
926	GCGCCGCGGCGGTG-GGGGTCGGGGGGG—G-GAGAGAAAGGGCCGA	Forward
927	CGCGGCGCCGCCAC-CCCCAGCCCCCCC-C-CTCTCTTTCCCGGCT	Reverse
930	GCGCGGCCCCGCGCCCCCAGC--------CACGGGAGCGGCGCCCCCGGGGCAACCCCCGCG	Forward
931	CGCGCCGGGGCGCGGGGGTCG--------GTGCCCTCGCCGCGGGGGCCCCGTTGGGGGCGC	Reverse
932	GCGCGGCCCCGCGCCCCCAGCAGAGCAGCACGGGAGCGGCGCCCCCGGGGCA	Forward
933	CGCGCCGGGGCGCGGGGGTCGTCTCGTCGTGCCCTCGCCGCGGGGGCCCCGT	Reverse
789	AGGCCTCGGACGCGTGGCGGGTGGAAGGCTCCGC	Forward
790	CTGCAGGCGTGTGGGAGCGACGCCGTCCGC	Reverse
791	AGGCCTCGGACACGTGGCGGGTGGAAGGCTCCGC	Forward

[a] Point mutations with respect to the wild-type sequence of vTR are highlighted in boldface gray shading, and deletion regions are represented by dashes.

TABLE II
Mutant construct elaboration

Constructs	1st PCR		2nd PCR
	Template	Primers[a]	Primers[a]
Mut23	pBMB 8–5	901/790	791/790
	pBMB 8–5	791/902	
dypvfc	pUC-cTR	905/790	791/790
	pBMB 8–5	791/904	
dcpvfc	pUC-cTR	905/790	789/790
	pBMB 8–5	789/904	
4pbc	pBMB 8–5	910/790	791/790
	pBMB 8–5	791/911	
1pbc	pBMB 8–5	914/790	791/790
	pBMB 8–5	791/915	
T/Gc	pBMB 8–5	918/790	791/790
	pBMB 8–5	791/919	
G/Ac	pBMB 8–5	922/790	791/790
	pBMB 8–5	791/923	
J2/3D	pBMB 8–5	924/790	791/790
	pBMB 8–5	791/925	
J2/3M	pBMB 8–5	926/790	791/790
	pBMB 8–5	791/927	
HD	pBMB 8–5	930/790	791/790
	pBMB 8–5	791/931	
HRI	pBMB 8–5	932/790	791/790
	pBMB 8–5	791/933	
HACABR	pBMB 8–5	770/790	790/791
	Risp	791/767	
J2/3rev	pBMB 8-5	901/790	789/790 (1)
	pUC-cTR	789/902	
	pUC-cTR (1)	907/790	789/790
		789/906	

[a] Primer sequences are described in Table I.

ACACGTGGCGGGTGGAAGGCT-3′) contains the start of the TR gene with a 5′-extension corresponding to the T7 RNA polymerase promoter (in *boldface*). The reverse primer M76 (5′-GCGTGTGGGAGCGACGC-CGT-3′) was used to amplify most TRs with the exception of ACA-mutated TRs, which were amplified with the reverse primer M75 (5′-GCGGGGAGCGACGCCGTCCG-3′), from which the ACA box was

specifically deleted. Fragments were amplified by PCR and purified as previously described (12).

In Vitro Transcription of Telomerase RNA—T7 *in vitro* transcription was carried out in a 200-μl reaction mixture containing 1 μg of PCR amplified or cTR DNA template, 1× T7 buffer (200 mM Tris-HCl, pH7.9, 50 mM NaCl, 30 mM $MgCl_2$, and 10 mM spermidine), 10 mM dithiothreitol, 1.5 units/μl RNasin (Promega), 4 mM ribonucleoside triphosphate, and 2 units/μl T7 polymerase (Promega) incubated at 37 °C for 2 h. The resulting RNA was treated with 10 units of RNase-free DNase I (Amersham Biosciences) at 37 °C for 15 min, and RNA was then extracted in phenol-chloroform with ethanol precipitation. The resulting pellet was suspended in 10 μl of RNase-free water (Promega). To standardize the assembly of the different transcribed TRs with TERT by minimizing variations of TR concentration, the amounts of TR were estimated with the Bio-profil 1D++ software (ChemiSmart 5000) from a 2% agarose gel run in Tris acetate EDTA buffer. The concentration of each TR then was adjusted to 1 μg/μl.

In Vitro Telomerase Reconstitution—The avian telomerase protein gene (chTERT) was expressed using the TnT system (Promega) according to the manufacturer's instructions. We assembled chTERT with the transcribed RNA as previously described (27). We incubated 0.75 μl of rabbit reticulocyte lysate reaction mixture containing the chTERT generated by *in vitro* translation at 30 °C for 2 h with 1 μg of *in vitro* transcribed RNA and 1× buffer E (50 mM NaCl, 20 mM HEPES, pH 8, 2 mM $MgCl_2$, 0.2 mM EGTA, 2 mM dithiothreitol, and 10% glycerol) in a final volume of 3 μl. Aliquots of ribonucleoprotein assembly products (3 μl of a 1:10 dilution in 1× buffer E) were used for the assessment of telomerase activity by telomere repeat amplification protocol (TRAP) assay.

TRAP Assay—Telomerase activity was assayed as previously described (12). Transiently transfected cells (48 h posttransfection) were trypsinized and washed twice with 1× phosphate-buffered saline. We then incubated 10^6 cells with 100 μl of ice-cold lysis buffer on ice for 30 min. The lysate was centrifuged at 12,000 × *g* for 30 min, and 80 μl of the protein-containing supernatant was removed and stored at −80 °C. We then determined the telomerase activity of 2 μg of cellular extract or 3 μl of the diluted *in vitro* ribonucleoprotein assembly mixture using the semiquantitative fluorescence-based TRAP assay (12). The PCR step was performed with TAMRA (6-carboxy-tetramethylrhodamine)-labeled forward primers TS (5′-AATCCGTGCAGCAGAGTT-3′) and CXext (5′-CCCTAACCCTAACCCTAACCCTAA-3′) as reverse primers. An internal amplification standard, required for the quantitative TRAP assay, was added to the PCR mixture and yielded a 135-bp product with the TS and CXext primers. Samples were analyzed by capillary electrophoresis (ABI Prism 310, PerkinElmer Life Sciences). The telomerase activity of each sample was quantified by adding the integrated value of the telomerase products (corresponding to telomerase hexamer repeats beyond the primer dimer peak) and as a function of the integrated value of internal amplification standard.

Each assay was performed at least three times. The mean ± S.D. for the activity of each construct was calculated, and the final results are expressed as a function of mean RB1B-vTR activity. Statistical analysis was performed with the non-parametric Kruskal-Wallis test implemented by Simstat, version 2.04 software (Provalis Research). The activities of the various constructs were independently compared with the mean activities of vTR (P/gv) or cTR (P/gc). p values ≤ 0.05 were considered to be statistically significant.

Quantification of Total and Nuclear RNA Accumulation—Total RNA was extracted from 10^6 transiently transfected cells with RNAble solution according to the manufacturer's instructions (Eurobio). We extracted nuclear RNA in a similar manner from nuclei prepared from transfected cells. The nuclei were isolated from 10^6 cells by incubating the cells with a 1% Nonidet P-40 solution on ice for 30 min. The suspension was then centrifuged at 14,000 × *g* for 30 min at 4 °C. The pellet containing the purified nuclei was resuspended in RNAble solution, and nuclear RNA was extracted. The accumulation of TR in cells and nuclei was quantified by fluorescence-based RT-PCR as previously described (12). The reverse transcription was performed with the DS4 primer (5′-AGCCCGCTGAAAGTCAGCGAGT-3′). PCRs were done from 2 μl of cDNA with the forward fluorescent-labeled primer TET-DS1 (5′-CGTGGCGGGTGGAAGGCTCCG-3′) and the reverse primer DS4. An internal amplification standard (pGEMTeasy-ICTR) required for the quantitative RT-PCR assay was added to the PCR mixture and yielded a 160-bp product with the DS1 and DS4 primers. The PCR products were detected by automated sequencing (ABI Prism 310). The expression of each TR was calculated as the ratio of the integrated value of the TR products on the ICTR-integrated value. Each assay was performed at least three times. The mean ± S.D. for the accumulation of each construct was calculated, and the final results were expressed as a function of mean RB1B-vTR accumulation. Statistical analysis was performed by means of the non-parametric Kruskal-Wallis test, implemented by Simstat, version 2.04 software. We compared the accumulation of constructs independently with the mean accumulation of RB1B-vTR (P/gv) or cTR (P/gc). p values ≤ 0.05 were considered to be statistically significant.

RESULTS

The Chicken TERT Is More Efficient with vTR Than with cTR—We cloned the 4038-bp cDNA of the chicken TERT from thymus cells extracted from the PA-12 White Leghorn chicken line. The sequence of this cDNA was found to be only moderately similar to its human and mouse counterparts as recently described (28). The messenger RNA for *chTERT* is nonetheless structurally similar to *hTERT* in comprising 16 exons, 10 of which (exons 3, 7–10, and 12–16) have identical lengths in both sequences with another 5 exons (exons 1, 4–6, and 11) slightly different (from 3 to 9 bp) (Fig. 2). The main divergences concerned the first two exons, encoding the N terminus of TERT. These two exons were significantly longer (by 57 and 570 bp, respectively) in *chTERT* than in *hTERT*. A comparison of the amino acid sequences of chTERT and hTERT led to the identification of seven reverse transcriptase motifs (1, 2, A, B, C, D, and E) in chTERT with various levels of identity to the corresponding motifs in hTERT (from 25 to 87%) with the B, C, D, and E most strongly conserved. The essential T motif, which specifies TERT telomerase activity, and the C-terminal end of the molecule responsible for enzyme processivity also displayed high levels of sequence identity (69 and 60% identity, respectively) between chTERT and hTERT. In contrast, the RID1 functional domain, which is involved in the interaction with TR and hTERT processivity, and the RID2 domain, which interacts with TR, presented much lower levels of amino acid conservation between the two TERTs (42 and 43%, respectively).

Based on levels of conservation of the functional domains, we checked the functionality of chTERT generated in a rabbit reticulocyte lysate system with *in vitro* transcribed vTR and cTR. In this homologous assay, we demonstrated that chTERT reconstituted an efficient telomerase complex with both TRs (Fig. 3). Furthermore, we found that vTR was 65% more efficient than cTR, whereas the negative control TEM construct consisting of the *vTR* gene deleted of its CR1 template region did not restore telomerase activity.

Mutations Affecting the P2 Helix and the Surrounding the P3 Helix Are Likely to Have Increased the Efficiency of vTR over That of cTR—The vTR nucleotide sequence diverges by 12% from that of cTR. Most mutations (50 of the 66 bp mutated) are located in the pseudoknot domain and confer much greater efficiency on vTR with both mTERT (12) and chTERT *in vitro*. Thus, we take advantage that vTR and cTR both interacts naturally with chTERT to estimate the contribution of the nucleotide divergence between vTR and cTR in the greater efficiency of vTR by introducing natural functional mutations occurring in the pseudoknot domain of cTR in a viral context.

Mutations affecting the pseudoknot domain can be gathered into two groups on the basis of their localization, mutations occurring in and around the P2 helix and mutations in the J2a/3 loop joining the P2 and the P3 helices (Fig. 4*A*). We independently tested the effect of the first group of mutations by the following: (i) introducing the 4-bp sequence (5′-CGCC-3′) specifically observed in the J2a/2b junction region of cTR, leading to the reconstitution of this region in vTR (4pbc construct); (ii) replacing the guanine of the P2a helix of vTR with the adenine present in the cTR sequence, resulting in a 1-base pair mismatch in this stem (G/Ac construct); (iii) replacing the uracil in the J2b/2a junction region of vTR with the guanine of cTR, resulting in base-pairing in the P2b helix of vTR (T/Gc con-

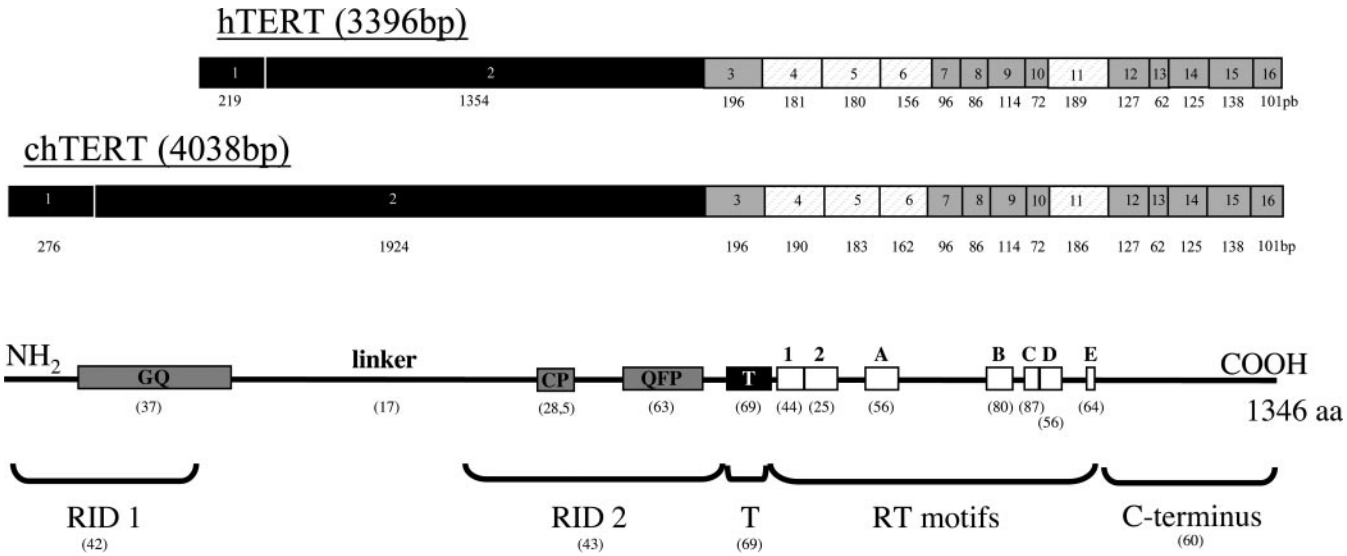

FIG. 2. **Genomic organization of the *chTERT* gene and its putative functional domains.** The 16 exons of the *chTERT* and *hTERT* cDNAs are represented as *boxes*, and their respective lengths are indicated below. The exons of identical length in *chTERT* and *hTERT* are shown *in* gray, exons slightly different in size (by 3–9 bp) are *hatched*, and exons differing significantly in length are shown in *black*. The putative functional domains of the chTERT protein were identified based on the organization of *hTERT* cDNA and are localized under the *chTERT* cDNA. The T motif is represented by a *black box* (amino acids 756–803), and the RT motifs are represented by *white boxes* (*motif 1*, amino acids 814–838; *motif 2*, amino acids 839–870; *motif A*, amino acids 915–948; *motif B*, amino acids 1038–1072; *motif C*, amino acids 1078–1092; *motif D*, amino acids 1095–1120; and *motif E*, amino acids 1139–1149). All were located as previously described (28). The GQ (amino acids 77–226), CP (amino acids 569–603), and QFP (amino acids 649–730) motifs are indicated by *gray boxes* (31). The RID1 (amino acids 46–170), RID2 (amino acids 515–757), and C-terminal (amino acids 1150–1346) domains are indicated below the diagram of the chTERT protein structure as previously defined for hTERT (18, 32).

struct); and (iv) introducing a uracil into the CR2 region of vTR downstream from the P2 helix (1pbc construct) (Fig. 4*B*). We also tested the overall effect of this group of mutations by specifically introducing the P2 helix of cTR into vTR (Mut23 construct). The second group of mutations concerns the J2a/3 loop of the vTR pseudoknot, which diverges from the nucleotide sequence of cTR by >80% due a deletion of 27 bp, 8 point mutations, and 8 insertions. We investigated the effects of these nucleotide divergences by means of a global approach based on three constructs combining various mutations. In the J2/3 M construct, we introduced all of the internal point mutations of the J2a/3 loop of cTR into vTR (four substitutions, G/U, UC/GU, C/G, and G/A, and the deletions of 2 adenines and 1 cytosine). The J2/3D construct contained the mutations specific to the 3′-end of the cTR J2a/3 loop: 1 A/G substitution and the deletion of 5 adenines surrounding a cytosine upstream from the P3 helix. Finally, the J2/3rev construct corresponds to the reverse construct of the whole J2a/3 loop, resulting in the introduction of the J2a/3 loop of vTR into the cTR context. It is worth stating that this construct is the only reverse construct used in this study on account of the inability to amplify the full-length J2a/3b loop of the *cTR* gene by PCR.

In the *in vitro* homologous assay, the first group of mutations affecting the P2 helix and its flanking sequences significantly decreased the telomerase activity of vTR, whatever the mutation considered (Fig. 5*A*). The introduction of the 4-bp sequence into the J2a/2b junction region of vTR (4pbc construct) reduced the telomerase activity of vTR to the level of cTR activity (43% WT-vTR activity). In contrast, the T/Gc, G/Ac, and 1pbc mutations had a lesser effect on vTR activity. Indeed telomerase activity of those constructs with chTERT is weaker than that with WT-vTR with chTERT (72, 58, and 54%, respectively) but significantly higher than that with cTR. Moreover, the overall effect of these mutations appeared to be cumulative, because the Mut23 mutant TR including all of the cTR P2 helix mutations described above reconstituted 34% WT-vTR activity, corresponding to a significant similar level to those with cTR.

Among the second group of mutations located within the J2a/3 junction region, the specific introduction of internal mutations of the cTR loop in vTR had no apparent effect on vTR telomerase activity (90% WT-vTR activity; $p > 0.05$). However, mutations in the 3′-end of this J2a/3 loop, especially the deletion of adenines upstream from the P3 helix, tended to decrease the vTR activity to the cTR level (48% WT-vTR activity). The reverse J2/3rev construct in which the J2a/3 loop of vTR was inserted into the *cTR* gene had no significant effect on cTR activity, underlying the dominant effect of the mutations in the pseudoknot region out of the J2a/3 loop.

In the heterologous cell assay, the whole mutated TR constructs gave significantly weaker telomerase activity than the wild-type vTR (from 43 to 78%; $p < 0.05$), regardless of the construct considered (Fig. 5*B*). However, only three mutations seemed to decrease vTR activity to cTR level: 1) the introduction of the uracil in the CR2 region of vTR (1pbc); 2) the G/A substitution within the P2 helix (G/A construct); and 3) the 3′-end mutations of cTR introduced in the J2a/3 junction of vTR (J2/3D construct). The telomerase activity of the other five mutant constructs, 4pbc, G/Ac, T/Gc, Mut23, and J2/3 M, was intermediate between and significantly different from vTR and cTR activities. Moreover, as observed in the homologous system assays, the introduction of the J2a/3 loop of vTR into cTR (J2/3rev construct) did not affect the cTR activity. These differences in telomerase activity are particularly relevant, because the mutations introduced had few or no significant effect on TR accumulation (Fig. 5*C*) since most mutated TRs are expressed to the wild-type vTR level.

Thus, the greater efficiency of vTR seems to be due to mutations occurring within the P2 helix, which may strengthen this stem, the deletion of the 4-bp sequence in the J2a/2b junction region particularly effective in this respect. Moreover, the only mutation affecting a conserved region (CR2) between vTR and cTR seems to increase the vTR activity as well as the 3′-end mutations located in the J2a/3 loop just upstream from the P3 helix. In contrast, the internal mutations of this J2a/3

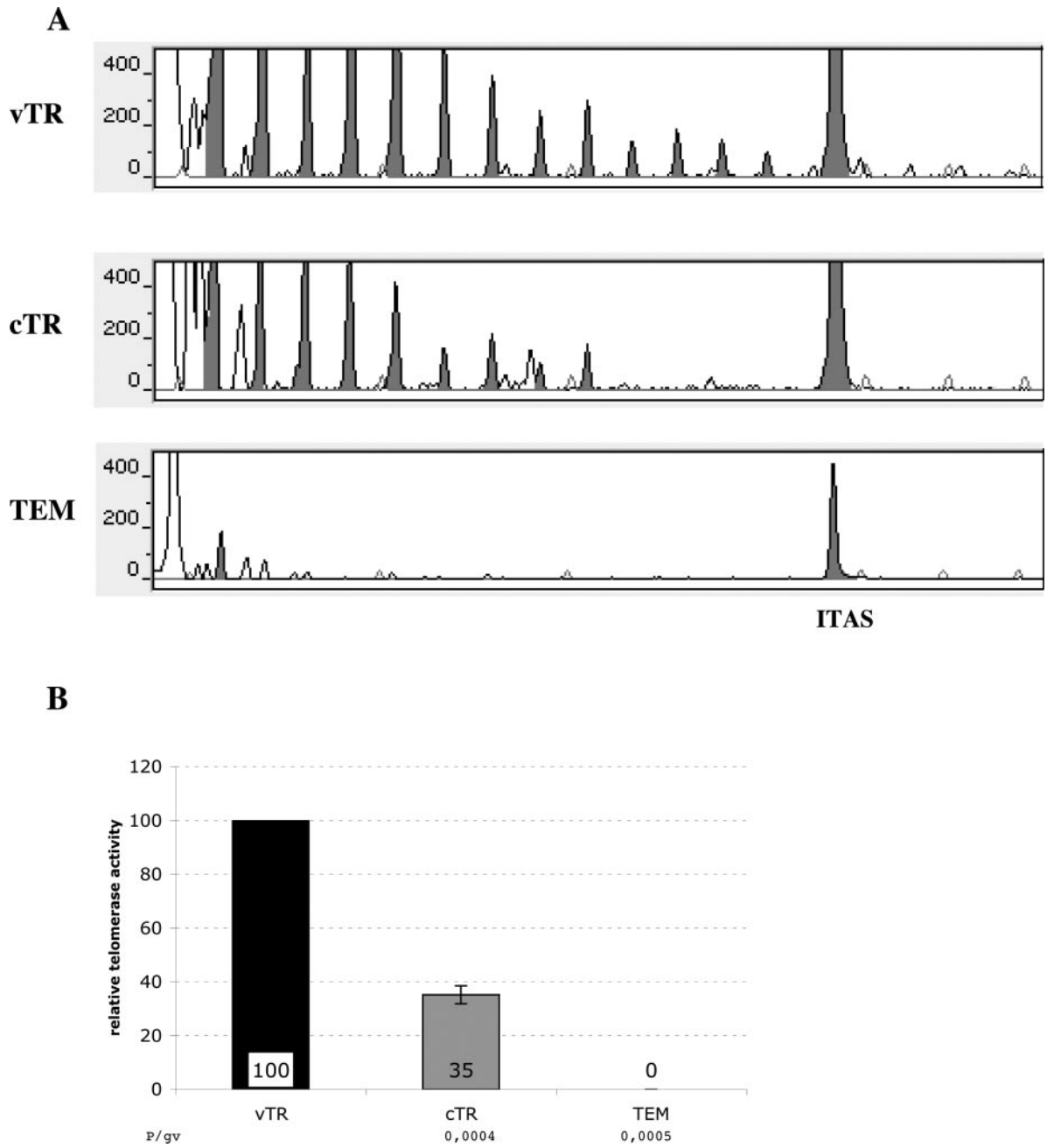

FIG. 3. **Reconstitution of telomerase activity in homologous *in vitro* assay.** The chTERT subunit was produced in a rabbit reticulocyte lysate system and assembled with *in vitro* transcribed vTR and cTR constructs and with the vTR mutant construct lacking the CR1 template region (TEM) as negative control. Each assembly was carried out three times in duplicate, and the resulting telomerase activity was measured by a modified TRAP assay based on the detection of fluorescent telomerase product on ABI Prism 310 (Applied Biosystems). *A*, classic electrophoregram profiles showing the 6-bp TRAP product for vTR, cTR, and the TEM construct. The position of the internal control (internal amplification standard (*ITAS*)) is indicated. *Filled-in areas* identify the 6-bp profile of the telomerase product. *B*, the telomerase activity reconstitution for each construct, calculated as previously described (12), is represented as a histogram with the mean ± S.D. represented by *bars*.

loop do not seem to be involved in the greater efficiency of vTR.

Mutations Located Outside the Pseudoknot Domain Make a Smaller Contribution to the Difference in Activity between vTR and cTR—As few mutations occurred between the start of the *vTR* gene and the pseudoknot domain (4 of the 66 mutations of the gene) or between the pseudknot domain and the 3′-end of the gene (11 mutations of the 66), we performed a global study to determine the relative roles of these mutations in increasing the activity of vTR. This approach consisted of testing chimeric constructs including the start of the cTR sequence (dcpvfv construct), the end of the cTR sequence (dvpvfc construct), and both the beginning and end of the cTR sequence (dcpvfc construct) in a viral context (Fig. 6*A*).

The chimeric constructs seem to reconstitute similar levels of telomerase activity, whether they were expressed in the heterologous assay or assembled with chTERT *in vitro*. Indeed, the three chimeric TRs, dcpvfv, dvpvfc, and dcpvfc, reconstituted 69–78% WT-vTR activity in cells and 76–86% WT-vTR activity with chTERT *in vitro*. These activities are significantly ($p < 0.05$) lower than those observed with the WT-vTR and higher than the cTR activity (Fig. 6*B*). Thus, the mutations at the start and end of the viral TR gene may be involved in increasing the efficiency of vTR but cannot account for the difference between vTR and cTR alone. It should be noted that all of the chimeras accumulated to levels similar to those for the *vTR* gene in KO3p23mTR$^{-/-}$ cells (82–95% WT vTR accumulation;

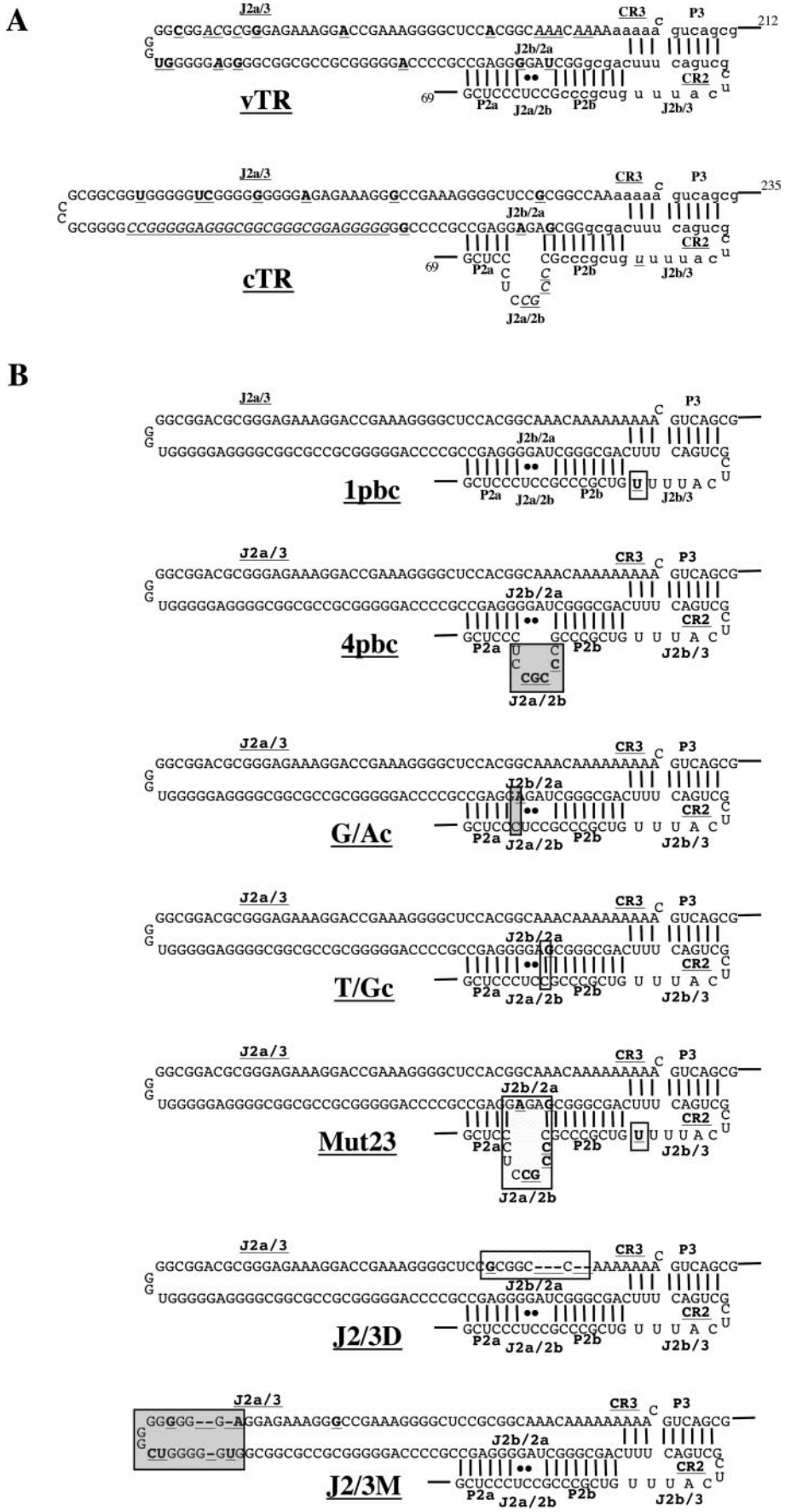

FIG. 4. **TR constructs mutated in the pseudoknot domain.** *A*, the pseudoknot domains of the wild-type vTR and cTR. Mutations between those two genes are indicated in *boldface underlined characters*, and deletions are indicated in *italicized underlined characters*. *B*, mutated constructs. Point mutations or groups of mutations are indicated by *gray boxes* with the mutations introduced shown in *boldface underlined characters* and the deletions shown as *dashes*.

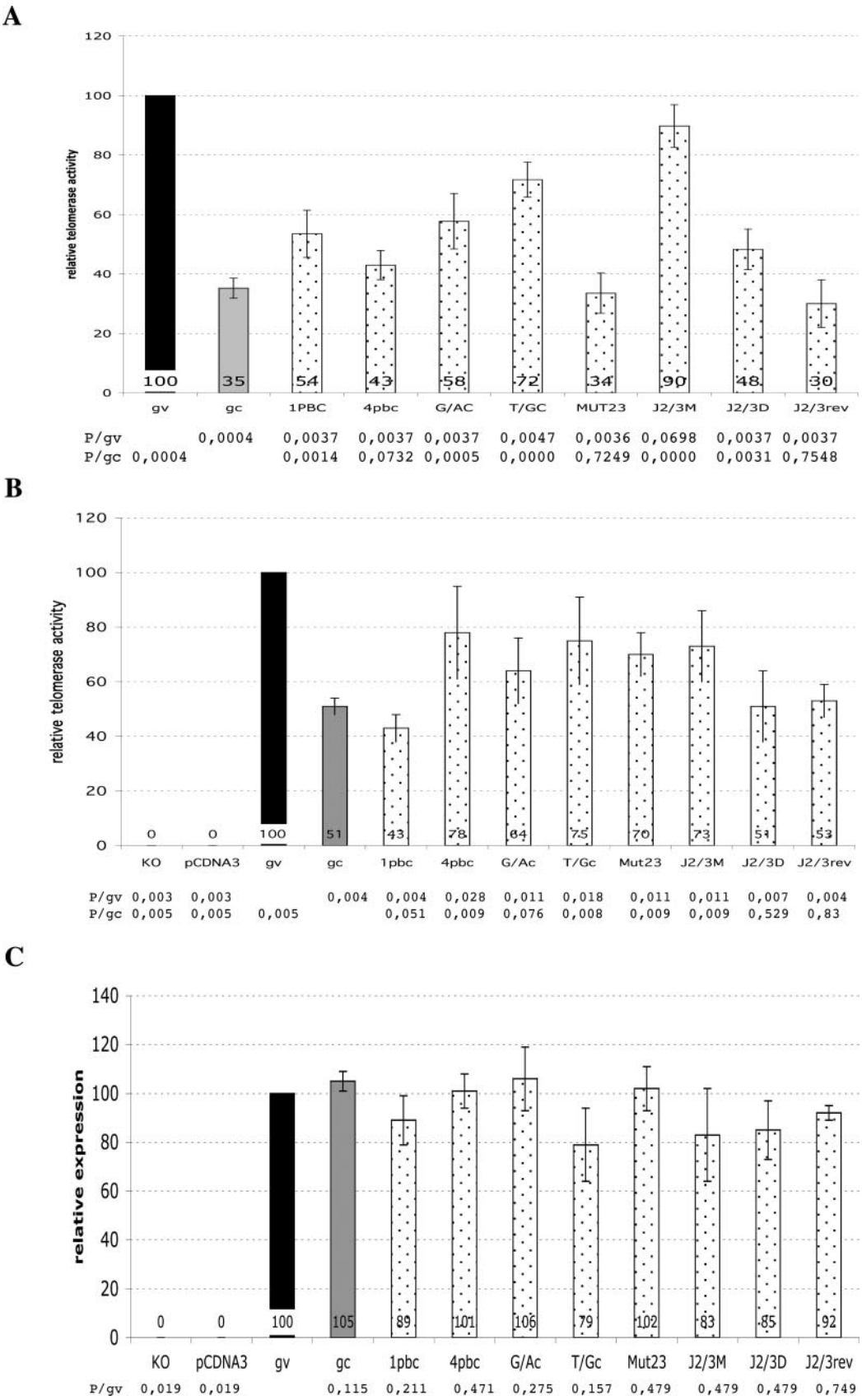

FIG. 5. **Involvement of individual mutations located in the pseudoknot domain in the telomerase activity and the accumulation of TR.** The wild-type *vTR* (gv) and *cTR* (gc) genes and constructs mutated in the pseudoknot domain were transcribed *in vitro* and assembled with the chTERT protein produced in a rabbit reticulocyte lysate system (*A*) or were used to transfect KO3p23mTR$^{-/-}$ cells transiently (*B* and *C*). The telomerase activity reconstituted in these two systems was then measured (*A* and *B*) by a modified TRAP assay based on the detection of fluorescent telomerase products on ABI Prism 310 and was expressed with respect to vTR activity (100%). In the heterologous system, TR expression in cells was quantified by RT-PCR following the extraction of total cellular RNA (*C*). Means ± S.D. are indicated by *bars*. The results of the Kruskal-Wallis statistical test comparing constructs to vTR (P/gv) and cTR (P/gc) are indicated below each histogram.

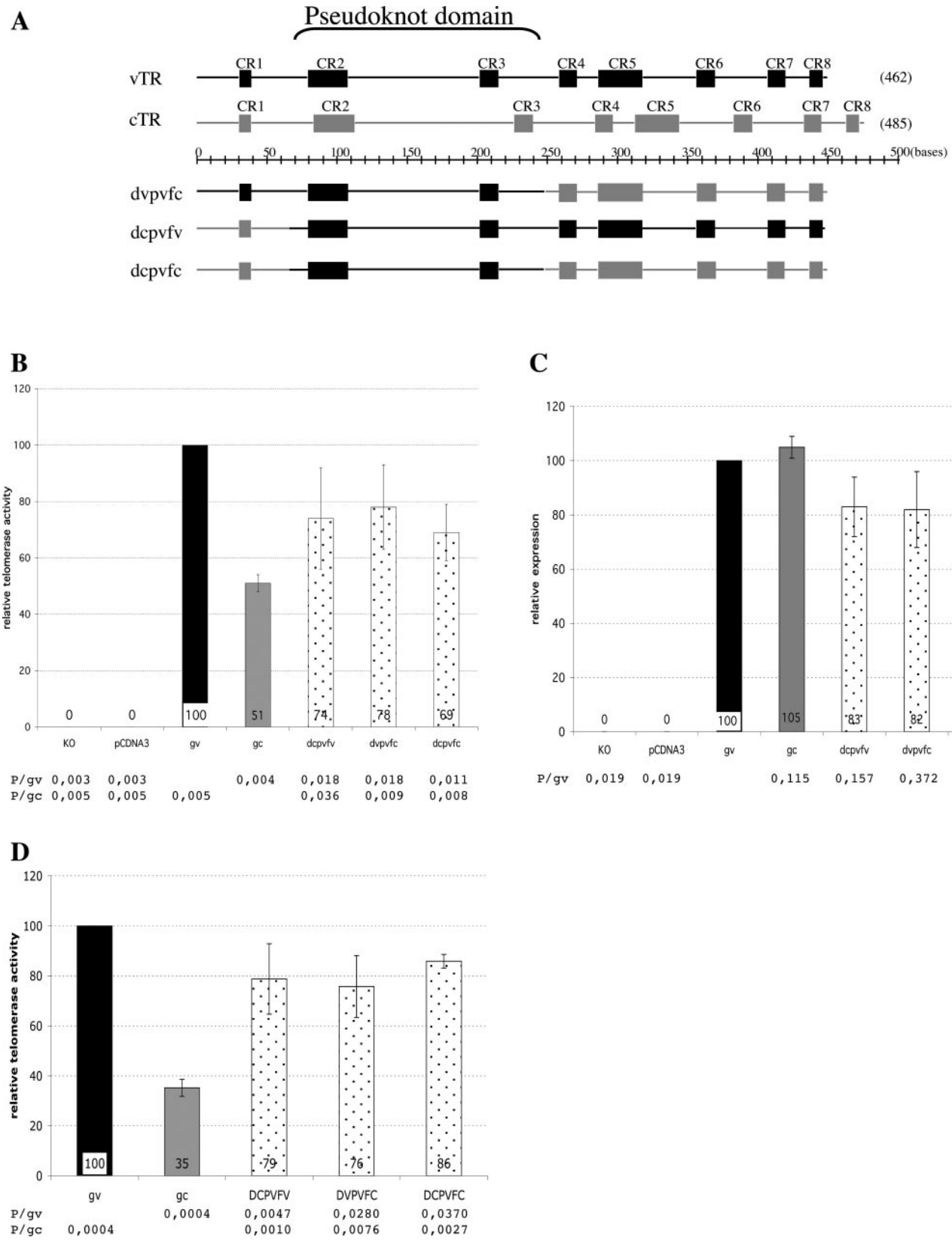

FIG. 6. **Effect of mutations outside the pseudoknot domain on telomerase activity and the accumulation of TR.** We assessed the overall effect of mutations located in the beginning and the end of vTR on its efficiency by producing chimeric constructs between vTR and cTR (*A*). The *vTR* gene (in *black*) and the *cTR* gene (in *gray*) are schematically represented with their conserved regions indicated as *boxes*. The chimeric constructs, shown under the nucleotide scale, consisted of the 5′-end and pseudoknot of vTR together with the 3′-end of cTR for the dvpvfc construct, the 5′-end of the *cTR* gene in a viral context for the dcpvfv construct, and the viral pseudoknot domain surrounded by cTR sequences for the dcpvfc construct. Those constructs were expressed in the heterologous KO3p23mTR$^{-/-}$ cell system. The restoration of telomerase activity was quantified (*B*), and TR expression in cells was checked by RT-PCR (*C*). These constructs were also tested in the homologous system by assembling the *in vitro* transcribed TRs and the expressed chTERT (*D*). Means ± S.D. are represented as *bars*. Results of the Kruskal-Wallis statistical test for comparisons with vTR (P/gv) and cTR (P/gc) are indicated below each histogram for each construct.

$p > 0.05$). This finding suggests that mutations occurring at the end of the vTR and the point mutation in the CR7 domain, in particular, have no effect on the vTR accumulation (Fig. 6*C*).

A One-nucleotide Mutation in the H-box of the Vaccine MDV-Rispens Strain vTR Induces a Defect of Telomerase Activity and Accumulation in Cells—As previously described (12), the alignment of the sequences of the vTRs of different MDV strains showed that the *vTR* gene of the vaccine MDV-Rispens strain differs from those of the other strains by three point mutations, especially a single substitution (A to G) at the 3′-end of the H-box (Fig. 7*A*). Thus, similarly explained in our report on the pseudoknot domains of vTR and cTR, we carried out a comparative functional study to estimate the effect of the "natural" mutations affecting the vTR of the vaccine MDV-Rispens strain compared with the vTR of the oncogenic MDV-RB1B strain. We first tested the native Rispens-vTR (Risp construct) to determine the global effect of the three mutations compared with the RB1B vTR and found that the Rispens-vTR reconstituted only 63% RB1B-vTR gene telomerase activity in KO3p23mTR$^{-/-}$ cells (Fig. 7*B*). According to the essential role for the telomerase activity *in vivo* of the H/ACA CR7 domain of vertebrate TR, since it includes consensus sequences conserved in all of the TRs of vertebrates, which are involved in the 3′-end processing of TRs and their nuclear accumulation in cells, we performed constructs for evaluating the specific role of the H-box mutation in the *vTR*-Rispens gene. Thus, we produced two constructs: one in which the H-box of the *vTR*-RB1B gene was replaced by the H-box of the vTR-Rispens (HRI construct) and one corresponding to its reverse construct, *i.e.* the H-box of the vTR-Rispens was replaced by the RB1B-vTR H-box (HACABR construct). We also used the HD, ACAD, and HACAD constructs in which the H-box, the ACA box, and both boxes, respectively, have been deleted as controls (Fig. 7*A*).

We took advantage of the cellular context provided by the heterologous mouse KO3p23mTR$^{-/-}$ to check the functionality of those different constructs and particularly their accumulation both in the whole cells and specifically in the nuclear fraction. At the same time, to abolish the accumulation effect and to test preferentially the proper activity of each TR, we tested those transcribed TRs with chTERT in the *in vitro* system.

As expected, the three control TRs restored telomerase activity only partially, if at all, in cells (0–11% WT-vTR activity), whereas their functionality did not seem to be altered, as shown by direct assembly *in vitro* (Fig. 7*C*), with the exception of the HACAD construct, which would be less efficient (61% RB1B-vTR). The weak activity observed in cells could be directly attributed to a defect in TR accumulation in cells (Fig. 7, *D* and *E*). Indeed, TR lacking the H-box accumulated less efficiently (57 and 71% in whole cells and nuclei, respectively) than RB1B-vTR, and the ACAD and HACAD TRs accumulated much less efficiently than the wild-type TR in whole cells (70 and 79%, respectively) and in the nucleus, in particular (2 and 7%, respectively).

With regard to the Rispens-vTR whose mutations would be less drastic than the deletion of functional boxes, the difference in telomerase activity observed in cells compared with the RB1B-vTR activity also seems to be also attributed to a loss of accumulation in the whole cell (50%) and especially in the nuclear compartment (60%) (Fig. 7, *D* and *E*) rather than due to decreases in functionality because the Rispens-vTR is as efficient (112%) as the RB1B-vTR *in vitro* (Fig. 7*C*). The only mutation affecting the H-box of the Rispens-vTR seems to be indeed responsible for the weaker telomerase activity of this TR, because replacement of the H-box of the RB1B-vTR by that of Rispens (HRI construct) induced the restoration of telomerase activity to levels similar to those obtained with Rispens-vTR (56% RB1B-vTR activity) (Fig. 7*B*). This loss of activity seems to be directly correlated with the 42 and 35% decreases in HRI-TR accumulation in total RNA and nuclear extracts, respectively, because the functionality of this TR was unaffected in *in vitro* assays (81% RB1B-vTR telomerase activity). Furthermore, the reverse construct, HACABR, in which the H-box of the Rispens-vTR was replaced by the RB1B-vTR H-box restored the Rispens vTR activity to the level of the RB1B vTR telomerase activity (89%) in cells as well as its accumulation level and restored accumulation both in whole cells and in the nuclear fraction (88 and 93% RB1B-vTR accumulation, respectively). Thus, it could be viewed that the lower efficiency of the Rispens-vTR in cells would rest on exclusively to the mutation affecting its H-box, which did not affect the functioning of the TR but instead led to defects in the accumulation and/or targeting of the TR.

DISCUSSION

This study, unlike most functional studies, which have used arbitrary deletions or mutations leading to a drastic loss of telomerase activity, is original in using a model based on the comparison of two active TR molecules. The vTR that we have identified in the genome of the Marek's disease virus and cTR display 12% divergence in nucleotide sequences, resulting in differences in telomerase activity. Thus, we used this "natural" model to determine, by introducing specific cTR mutations in a viral context, the functional regions of vTR and to identify nucleotide differences responsible for the greater efficiency of vTR than that of cTR. This study was first performed in a heterologous system, based on the reconstitution of telomerase activity, expressing our mutant TRs in cells producing the murine TERT. This system, classically used in functional TR studies, makes it possible to evaluate the expression and accumulation of the mutant TR in a cellular context and allow the assembly of these TR with a TERT molecule that tolerates sequence variation in TR (17). The cloning of the chicken TERT cDNA led us to demonstrate by a *in vitro* assay that vTR and cTR are also able to take part to an efficient telomerase complex with their natural homologous protein subunit chTERT. Furthermore, the chTERT·vTR complex seems to be three times as efficient as the chTERT·cTR complex. It is noteworthy that this difference in efficiency was therefore less marked in the heterologous system (about double), potentially consistent with the mTERT subunit being more tolerant or with additional effects of cellular posttranscriptional steps.

We previously have shown (12) that the main mutations resulting in sequence differences between vTR and cTR are located in the pseudoknot domain. This domain, which is highly conserved in the TR of vertebrates, plays a key role in telomerase activity, because it mediates the dimerization of the TR and, together with the CR4/CR5 domain, constitutes a site of interaction with TERT (14, 18). Among the three helices that composed the pseudoknot domain, the second helix (P2) of vTR is split up into two stems, the P2a and P2b helices, joined by the J2a/2b and J2b/2a junction regions. Based on the mutations occurring in P2, this region of vTR is characterized by a global reinforcement of the structure compared with cTR. The deletion of the 4 bp in the J2a/2b junction region of vTR is likely to stabilize the vTR P2 helix, because the specific introduction of this sequence into vTR resulted in telomerase activity levels similar to those of cTR after assembly with chTERT. Similar results were obtained following deletion of the J2a.1/2a junction region from mTR, leading to a 130% increase in activity (29). The vTR pseudoknot structure and the P2 helix, in particular, may also be strengthened by the G/A mutation in the J2b/2a junction region of vTR, creating a conventional base-

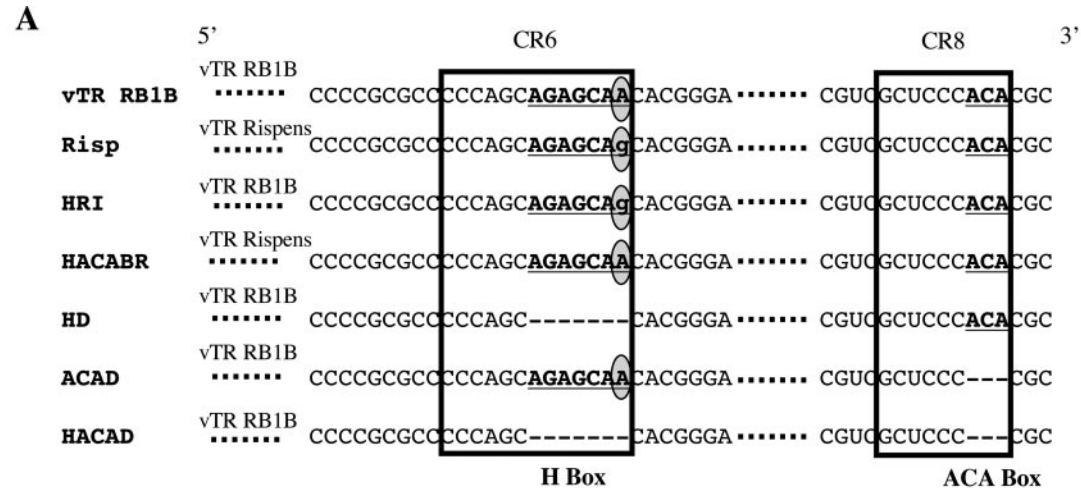

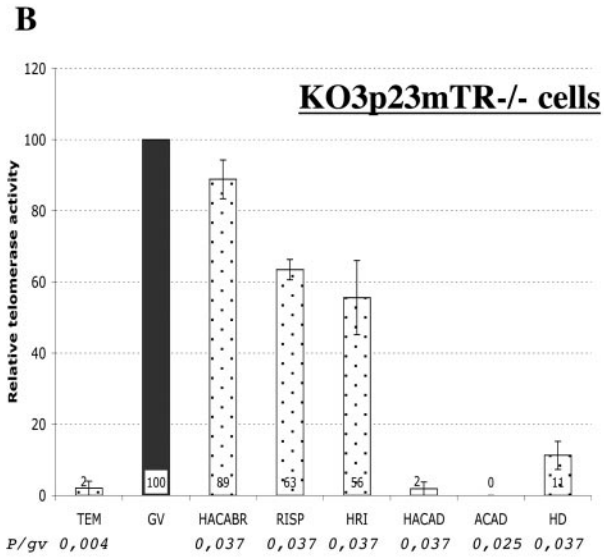

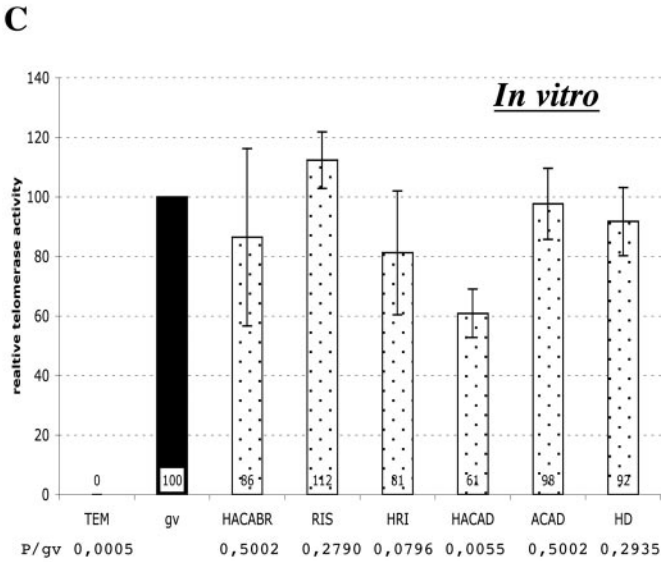

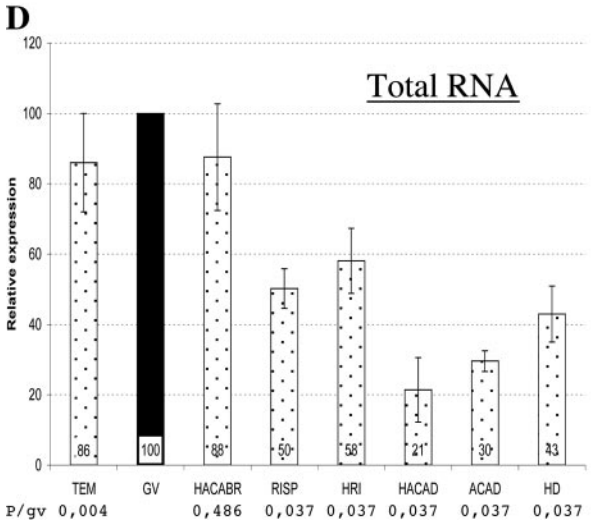

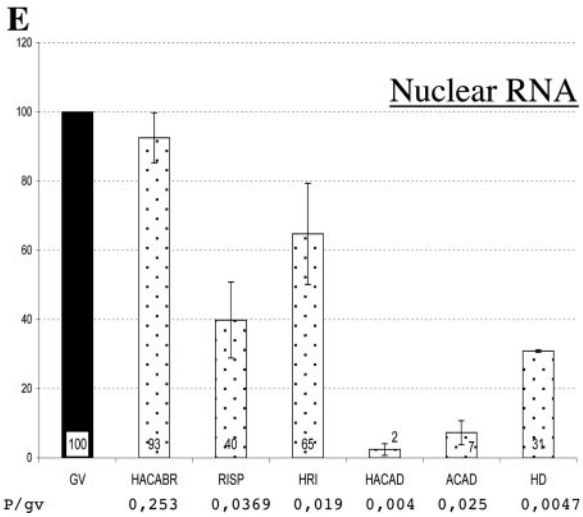

FIG. 7. **Functional study of the H/ACA boxes of vTR.** *A*, the H and ACA boxes of the vTR of the oncogenic MDV-RB1B and vaccine MDV-Rispens strains are indicated in *boldface underlined* characters. The natural single-nucleotide mutation of the H-box of the Rispens-vTR strain is *encircled* in *gray*. The mutagenesis TR constructs corresponding to the specific replacement of the RB1B-vTR H-box by the Rispens-vTR H-box (HRI construct) and the reverse construct (*i.e.* replacement of the Rispens-vTR H-Box by the RB1B-vTR H-Box (HACABR construct)) are represented below. The control constructs HD, ACAD, and HACAD, corresponding to the deletion of the H-box, the ACA-box, or both, respectively, are represented below. *B–E*, functional comparative study of the H/ACA domains of two *vTR* genes. The ability of the RB1B-vTR, Rispens-vTR, and associated mutated and control constructs to reconstitute telomerase activity was assessed in the heterologous system (*B*) and by *in vitro* assembly with chTERT (*C*). Telomerase activity was measured by a modified TRAP assay based on fluorescence. The level of expression of the different TR was quantified in transfected KO3p23mTR−/− cells and, specifically, in cell nuclei by RT-PCR assays following the extraction of total and nuclear RNA (*D* and *E*, respectively). Means ± S.D. are represented as *bars*. Results of the Kruskal-Wallis statistical test for comparison with vTR (P/gv) are indicated below each histogram for each construct.

pairing at the 3′-extremity of the P2a helix. This was demonstrated by replacing the substituted residue of the vTR with the residue present in the P2a helix of cTR, which led to 36 and 42% decreases in telomerase activity with the mTERT and chTERT subunits, respectively. Conversely, the strengthening of the P2b helix by a conventional base-pairing in cTR (T/Gc construct) appeared to have no effect on cTR activity, because the introduction of this mutation in vTR did not increase telomerase activity, regardless of the system used. Thus, the structure of the P2 helix and the P2a helix, in particular, appears to be essential for telomerase activity, as reported for the hTR pseudoknot in which the specific substitution of the upper or lower strand of the helix abolishes telomerase activity (19).

Another highly important structure within the pseudoknot domain of vertebrates is the P3 helix, which constitutes the dimerization interface between the two copies of TR in the telomerase complex. A recent study (18) reported that indeed each strand of the P3 helix of hTR would belong to two distinct hTR molecules, thereby stabilizing hTR dimer structure within the telomerase complex. The P3 helices of vTR and cTR are strictly identical in the primary sequence and therefore in the structure to the P3 helices of the well characterized hTR and mTR subunits (13) for which the solely structural importance of this helix in telomerase activity has been demonstrated in deletion and substitution studies (19). However, the regions surrounding the P3 helix of vTR and cTR present nucleotide divergences, which seem to be important on the efficiency of vTR according to our results. First, the deletion of a single nucleotide in the vTR CR2 region (the only nucleotide difference in a conserved region between vTR and cTR) within the J2b/3 junction region was examined. The introduction of a uracil into the vTR CR2 region induced a decrease of telomerase activity in both the heterologous and homologous systems with the mutant vTR (1pbc) restoring only 43 and 54% WT-vTR telomerase activity. This is consistent with the recent observation that, in the hTR pseudoknot, replacement of the three uracil residues of J2ab/3 by three guanines abolishes the ability of hTR to reconstitute an active telomerase complex (19). Secondly, several internal mutations were identified in the J2a/3 junction region and a deletion of five adenines at the 3′-extremity of this junction upstream from the P3 helix was observed in the vTR pseudoknot. A functional role of the sequence located upstream from the P3 helix at the 3′-extremity of the J2a/3 helix was first reported in hTR studies (17). It should be noted that the organization of this region in vTR, cTR, mTR, and hTR shows that the vTR sequence (5′-CGGC**AAACAA**AAAA-3′) is strikingly similar to that of hTR (5′-GAGC**AAACAA**A-3′), whereas the cTR sequence (5′-CGGCCAAAA-3′) is more similar to that of mTR (5′-CGAGCCUCAAAAA-3′) (13). Our functionality assays demonstrated that deletion of the five adenines surrounding the cytosine (shown above in *boldface* and *underlined*) in vTR significantly decreased telomerase activity by 50%, regardless of the TERT used in the reconstitution assay. This is consistent with previous reports in which replacement of the three adenines located at the extremity of the hTR J2a/3 junction region with three cytosines led to a loss of telomerase activity (19) as did the replacement of the 7-bp sequence located just upstream from the P3 helix of hTR (5′-AAACAAA-3′) with the mTR sequence (17). Conversely, internal sequences in the J2a/3 junction regions seem to have a weak effect on telomerase activity as described for hTR (17), because introducing cTR-specific mutations in the vTR J2a/3 sequence led to a weak decrease of telomerase activity compared with the WT-vTR (73 and 54% activity in the heterologous and homologous assays, respectively). Therefore, this study confirms previous data on hTR and mTR, indicating that adjacent sequences of the P3 helix would play a key role in telomerase activity. Given the role of this helix in TR dimerization, it would be conceivable that the deletion of the adenines in the cTR J2a/3 junction region could led to an unfavorable structure of the pseudoknot domain in cTR, resulting in poor stabilization of cTR dimerization and impairing interactions with TERT. A recent study (30) shows that an antisense oligonucleotide targeting 16 nucleotides of the J2a/3 loop of hTR, including the first three adenines of the 5′-AAACAAA3′ sequence, caused a 26% decrease in telomerase activity *in vitro* and an increase in hTR-DNA telomeric sequence complex formation (30). These data would indicate first a potential cumulative effect of the whole adenines of this region on the TR activity itself or on dimerization and second that the lower efficiency of cTR than vTR would rest on a lower processivity of the TERT·cTR complex due to a more stable binding of cTR to telomeric sequences.

The functionality of the telomerase complex *in vivo* depends directly on the accumulation, processing, and stability of TR in the cell nucleus. These properties are conferred by the H/ACA-CR7 domain. The requirement for this domain has been documented, particularly in terms of mutations affecting this domain in human diseases such as aplastic anemia and dyskeratosis congenita. Our results add to previous data concerning the H/ACA domain, because we carried out a functional study in a second "natural" model based on the appearance of a single-nucleotide mutation within the H-box of the vaccine MDV-Rispens strain vTR. We showed that the lower efficiency of MDV-Rispens vTR to reconstitute telomerase activity (63% of that obtained with the vTR encoded by the oncogenic MDV-RB1B strain) in the heterologous system would result only from the single mutation affecting its H-box. This mutation would indeed impair the accumulation of this TR in cells, particularly in the nucleus, that could be correlated to the decrease in the telomerase activity observed.

We also confirmed that the H/ACA domain of vTR was essential in a functional study based on the drastic deletion of the consensus sequences H and ACA. We showed that the loss of ability of vTR mutants from which H- and/or ACA boxes had been deleted to reconstitute efficient telomerase activity was directly linked to the very low levels of TR accumulating in cells, because their functionality was not altered. It is noteworthy that the deletion of both the H- and ACA boxes induced nonetheless a weak decrease of telomerase activity *in vitro* (61% activity), possibly due to poor processing of the 3′-end of the mutant TR. We also confirmed that the targeting of vTR to the nucleus was essential, as it reported for hTR, and that this targeting was linked to the functionality of the ACA box because the deletion of this box leads to a 98% decrease in the nuclear accumulation of vTR, whereas 30% was still detected in the total RNA fraction. Conversely, although deletion of the H-box leads to a decrease in vTR accumulation in total extract, most of the RNA detected is found in the nucleus. Thus, the H-box of vTR seems more likely to be involved in nucleolar targeting as previously shown for hTR (20, 21).

In conclusion, our results confirm the structural importance of the P2 helix of the pseudoknot domain of TRs and suggest a key role for the sequences surrounding the P3 helix. Moreover, we showed by means of a functional approach that telomerase activity can be directly correlated with the accumulation and nuclear targeting of TRs in cells. However, it is now essential to consider the dynamics of the multimeric telomerase complex and to investigate the extent to which vTR and cTR are able to form homodimers and heterodimers. We also need to assess the importance of such dimerization in interactions with chTERT and, more globally, in telomerase processivity.

Acknowledgments—We thank members of the VBE laboratory for critical comments on this study and especially Evelyne Esnault for assistance in the maintenance of cell cultures.

REFERENCES

1. Zakian, V. A. (1995) *Science* **270,** 1601–1607
2. Blackburn, E. H. (2000) *Nature* **408,** 53–56
3. Blackburn, E. H. (2001) *Cell* **106,** 661–673
4. Greider, C. W., and Blackburn, E. H. (1989) *Nature* **337,** 331–337
5. Hiyama, K., Hirai, Y., Kyoizumi, S., Akiyama, M., Hiyama, E., Piatyszek, M. A., Shay, J. W., Ishioka, S., and Yamakido, M. (1995) *J. Immunol.* **155,** 3711–3715
6. Wright, W. E., Piatyszek, M. A., Rainey, W. E., Byrd, W., and Shay, J. W. (1996) *Dev. Genet.* **18,** 173–179
7. Kim, N. W., Piatyszek, M. A., Prowse, K. R., Harley, C. B., West, M. D., Ho, P. L., Coviello, G. M., Wright, W. E., Weinrich, S. L., and Shay, J. W. (1994) *Science* **266,** 2011–2015
8. Shay, J. W., and Bacchetti, S. (1997) *Eur. J. Cancer* **33,** 787–791
9. Oh, S. T., Kyo, S., and Laimins, L. A. (2001) *J. Virol.* **75,** 5559–5566
10. Chen, Z., Smith, K. J., Skelton, H. G., III, Barrett, T. L., Greenway, H. T., Jr., and Lo, S. C. (2001) *Exp. Biol. Med.* **226,** 753–757
11. Okubo, M., Tsurukubo, Y., Higaki, T., Kawabe, T., Goto, M., Murase, T., Ide, T., Furuichi, Y., and Sugimoto, M. (2001) *Cancer Genet. Cytogenet.* **129,** 30–34
12. Fragnet, L., Blasco, M. A., Klapper, W., and Rasschaert, D. (2003) *J. Virol.* **77,** 5985–5996
13. Chen, J. L., Blasco, M. A., and Greider, C. W. (2000) *Cell* **100,** 503–514
14. Bachand, F., and Autexier, C. (2001) *Mol. Cell. Biol.* **21,** 1888–1897
15. Kim, M. M., Rivera, M. A., Botchkina, I. L., Shalaby, R., Thor, A. D., and Blackburn, E. H. (2001) *Proc. Natl. Acad. Sci. U. S. A.* **98,** 7982–7987
16. Ware, T. L., Wang, H., and Blackburn, E. H. (2000) *EMBO J.* **19,** 3119–3131
17. Chen, J. L., and Greider, C. W. (2003) *EMBO J.* **22,** 304–314
18. Moriarty, T. J., Marie-Egyptienne, D. T., and Autexier, C. (2004) *Mol. Cell. Biol.* **24,** 3720–3733
19. Ly, H., Blackburn, E. H., and Parslow, T. G. (2003) *Mol. Cell. Biol.* **23,** 6849–6856
20. Lukowiak, A. A., Narayanan, A., Li, Z. H., Terns, R. M., and Terns, M. P. (2001) *RNA* **7,** 1833–1844
21. Narayanan, A., Lukowiak, A., Jady, B. E., Dragon, F., Kiss, T., Terns, R. M., and Terns, M. P. (1999) *EMBO J.* **18,** 5120–5130
22. Marrone, A., and Mason, P. J. (2003) *Cell Mol. Life Sci.* **60,** 507–517
23. Mason, P. J. (2003) *BioEssays* **25,** 126–133
24. Blasco, M. A., Lee, H. W., Hande, M. P., Samper, E., Lansdorp, P. M., DePinho, R. A., and Greider, C. W. (1997) *Cell* **91,** 25–34
25. Autexier, C., and Greider, C. W. (1998) *Nucleic Acids Res.* **26,** 787–795
26. Joubert, P., Pautigny, C., Madelaine, M. F., and Rasschaert, D. (2000) *J. Gen. Virol.* **81,** 481–488
27. Mitchell, J. R., and Collins, K. (2000) *Mol. Cell* **6,** 361–371
28. Delany, M. E., and Daniels, L. M. (2004) *Gene* (*Amst.*) **339,** 61–69
29. Martin-Rivera, L., and Blasco, M. A. (2001) *J. Biol. Chem.* **276,** 5856–5865
30. Yeo, M., Rha, S. Y., Jeung, H. C., Shen, X. H., Yang, S. H., An, S. W., Roh, J. K., and Chung, H. C. (2005) *FEBS Lett.* **579,** 127–132
31. Xia, J., Peng, Y., Mian, I. S., and Lue, N. F. (2000) *Mol. Cell. Biol.* **20,** 5196–5207
32. Moriarty, T. J., Huard, S., Dupuis, S., and Autexier, C. (2002) *Mol. Cell Biol.* **4,** 1253–1265